

Dynamical analyses of the companions orbiting eclipsing binaries II. Z Draconis with four companions close to 6:3:2:1 mean motion resonances

Jinzhao Yuan¹, Hakan Volkan Şenavcı², Juanjuan Liu³, Selim O. SELAM²

and Damla GÜMÜŞ²

¹*Department of Physics, Shanxi Normal University, Linfen 041004, Shanxi, China (yuanjz@sxnu.edu.cn)*

²*Department of Astronomy and Space Sciences, Ankara University, Faculty of Science, TR-06100 Tandoğan-Ankara, Turkey*

³*Qiaoli Middle School, 041072 Linfen, Shanxi Province, China*

12 November 2018

ABSTRACT

All available mid-eclipse times of the short-period eclipsing binary Z Draconis are analysed, and multiple cyclic variations are found. Based on the light-travel time model, we find three companions around Z Draconis, and one or more possible short-period companions. The derived orbital periods suggest that the three outer companions and an inner one are in a near 6:3:2:1 mean-motion resonances. The most outer companion has the minimum mass of $\sim 0.7M_{\odot}$, whereas other companions are M dwarfs. We have studied the stabilities of the companions moving on a series of mutually inclined orbits. The results show that no orbital configurations can survive for 200 yr. We speculate that the instability of the system can be attributed to the uncertainties of the short-period companions, which result from the low-precision mid-eclipse times. Thus, secular CCD observations with much higher precision are needed in the future.

Key words: binaries: close – stars: individual: Z Draconis – methods: numerical.

1 INTRODUCTION

The oscillations in the mid-eclipse times of eclipsing binaries are usually interpreted as the light-travel time (LTT) effect via the presence of the companion orbiting around the eclipsing pair. Obviously, the multi-periodic variations in the eclipse times of an eclipsing binary provide us important constraints on the orbital characteristics of this multi-companion system, which comprises an eclipsing binary and multiple sub-stellar objects or planets.

Z Draconis (BD+73°533 = HIP 57348, $V_{max} = 10.67$ mag) was first found to be an Algol-type binary (hereafter Z Dra AB) by Ceraski (1903). Due to its high declination and brightness, abundant photometric data were obtained by small telescopes with alt-azimuthal mountings. Dugan (1915) conducted a detailed period study of the system and found that the mid-eclipse times show two sinusoidal variations with periods of 11.0 and 27.4 yr, while Giuricin, Mardirossian & Mezzetti (1983) found only one cyclic period of 20.3 yr. The first radial velocity curve for the primary component was obtained by Struve (1947). Based on the radial velocity curve and the *BVRI* light curves obtained with a 0.25 Schmidt-Cassegrain telescope, Terrell (2006) carried out a simultaneously photometric analysis.

In this paper, the timing variations of Z Dra are re-

analysed, and the orbital parameters of multiple companions are presented. Finally, the dynamical evolutions of the companions in all possible orbital inclinations are simulated.

2 ECLIPSE-TIMING VARIATIONS AND LTT MODEL

We carried out the CCD observations of Z Dra at the Ankara University Kreiken Observatory (AUKR-T40) in 2014 April 27 using the 40-cm Schmidt-Cassegrain telescope, equipped with an Apogee ALTA U47 + 1k × 1k CCD camera. The standard Johnson-Cousin *BVR_cI_c* filters were used in an alternating manner. The integration time for each image was 60 s in the *B* band, 30 s in the *V* band, 20 s in the *R_c* band, and 15 s in the *I_c* band. The readout time of the CCD camera was about 5 s. Over the course of the observing run, the weather condition was suitable for such a photometric observation with intermittent clouds seen around horizon. We fit the transit center of the eclipse in each band by using the technique of Kwee & van Woerden (1956), giving mid-eclipse times $\text{HJD}2456775.4605 \pm 0.0002$ in the *B* band, 2456775.4605 ± 0.0002 in the *V* band, 2456775.4602 ± 0.0002 in the *R_c* band, and 2456775.4603 ± 0.0002 in the *I_c* band.

One mid-eclipse time, HJD 2456775.4604 \pm 0.0002, was obtained by averaging those in the four bands.

The Lichtenknecker Database of the BAV¹ and the O-C Gateway Database² list all available mid-eclipse times of Z Dra in the literature. In addition, 15 mid-eclipse times between 1928 and 1949 were obtained by Kreiner, Kim & Nha (2001) and kindly sent to us (private communication). In total, we have collected 816 mid-eclipse times, which have a time span of 124 yr. All the data are listed in Table 1, and the corresponding $O - C$ values (see below) are plotted in Fig. 1. As shown in Fig. 1, 10 visual and photographic times are discarded for their large deviation from the $O - C$ curve. Furthermore, four times (HJD 2422918.37438, 2422933.30738, 2423499.35938, and 2423757.27438) deviate from all fits (see below) by more than 0.01 d. Finally, the remaining 802 data are used for our analyses.

Most mid-eclipse times were published without uncertainties. Therefore, a probable uncertainty of $\sigma = \pm 0.0002$ d is assumed for the photoelectric and CCD data, and ± 0.005 d for the photographic, plate and visual data. The uncertainty of ± 0.0003 d is adopted if it is less than ± 0.0003 d. The secondary eclipse times, HJD 2456601.0307 and 2455570.7246, show deviations as large as ± 0.003 d from the $O - C$ curve, which are larger than the published uncertainty of $\sigma = \pm 0.0006$ d. For the same reason, the uncertainty of ± 0.001 d is adopted for four CCD primary eclipse times (HJD 2453266.4698, 2453445.6484, 2454200.3792, and 2455700.3583), and ± 0.002 d for other five CCD primary eclipse times (HJD 2453817.5865, 2453847.4461, 2455329.7709, 2456039.7220, and 2456601.0315). Eventually, all high-precision (i.e., $\sigma < 0.001$ d) data spread over the last 15 yr, and most low-precision (i.e., $\sigma \geq 0.001$ d) data over the remaining time.

Since the Heliocentric Julian Dates (HJD) in Coordinated Universal Time (UTC) system are not uniform, all eclipse times after 1950 have been converted to Barycentric Julian Dates (BJD) in Barycentric Dynamical Time (TDB) system using the UTC2BJD³ procedure provided by Eastman, Siverd & Gaudi (2010). For the eclipse times before 1950, the relation between the Universal Time (UT) and the Terrestrial Time (TT) given by Duffett-Smith & Zwart (2011) is adopted for the conversion, producing additional uncertainties of a few seconds, which are much smaller than their assumed uncertainty of 0.005 d (i.e., 432 s).

Based on the eclipse times between 2011 and 2014, a new linear ephemeris

$$\text{Min } I = \text{HJD}2456775.4605 + 1^{\text{d}}.35745406 \times E \quad (1)$$

is obtained for future observations. In this paper, the eclipse-timing residuals, $O - C$, are computed with respect to the linear ephemeris given by Kreiner, Kim & Nha (2001),

$$\text{Min } I = \text{BJD}2443499.7305 + 1^{\text{d}}.35743190 \times E, \quad (2)$$

where E denotes the cycle number. The $O - C$ data is displayed in Fig. 1.

Comparing with binary evolutionary timescales, the 124 yr baseline is infinitely short. So, the mass transfer rate in

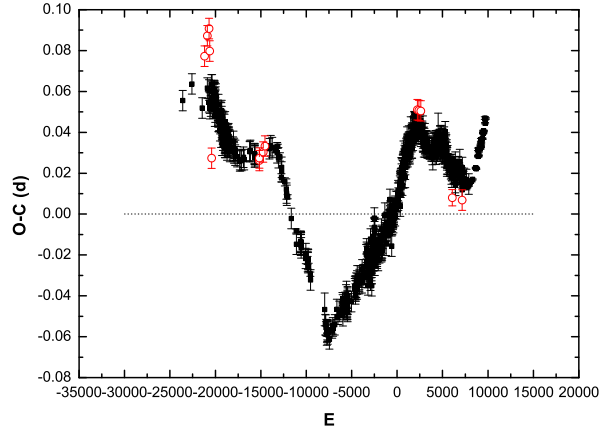


Figure 1. The $O - C$ diagram of Z Dra. The (black) filled squares refer to the useful data, and (red) open circles to the discarded data. Note that the error bars are smaller than the filled squares for the high-precision data in the last 4000 cycles. (A color version of this figure is available in the online journal.)

the eclipsing pair should change little or remain constant over the past 124 years, suggesting a continuous observed period increase. Therefore, we use an ephemeris including a quadratic term and one LTT term (Irwin 1952) to fit the $O - C$ values:

$$(O - C)(E) = T_O(E) - T_C(E) = C_0 + C_1 \times t + C_2 \times t^2 + \frac{a_3 \sin i_3}{c} \left[\frac{1 - e_3^2}{1 + e_3 \cos \nu_3} \sin(\nu_3 + \omega_3) + e_3 \sin \omega_3 \right], \quad (3)$$

where t is the eclipse time (minus BJD2400000) corresponding to the cycle number E , and $a_3 \sin i_3$ is the projected semi-major axis of the eclipsing pair around the barycentre of the triple system (i_3 is the orbital inclination of the companion with respect to the tangent plane of the sky). In equation (3), e_3 is the eccentricity, and ω_3 is the argument of the periastron measured from the ascending node in the tangent plane of the sky. ν_3 is the true anomaly, which is related with the mean anomaly $M = 2\pi(t - T_3)/P_3$, where T_3 and P_3 are the time of the periastron passage and orbital period, respectively.

For fixed e_3 , T_3 , and P_3 , ν_3 at all mid-eclipse times can be computed. Then, we fit the $O - C$ data with equation (3), and get the goodness-of-fit statistic, χ^2 , which is the weighted sum of the squared difference between the $O - C$ values y_i and the model values $y(t_i)$ at eclipse times t_i :

$$\chi^2 = \sum_{i=1}^{802} \left[\frac{y_i - y(t_i)}{\sigma_j} \right]^2 = W \sum_{i=1}^{802} w_i [y_i - y(t_i)]^2, \quad (4)$$

where

$$w_i = \frac{1}{W} \frac{1}{\sigma_i^2}, \quad (5)$$

and

$$W = \sum_{j=1}^{802} \frac{1}{\sigma_j^2} = 7.11 \times 10^8 \text{ d}^{-2}. \quad (6)$$

¹ <http://www.bav-astro.de/index.php?sprache=en>

² <http://var.astro.cz/ocgate/>

³ <http://astroutils.astronomy.ohio-state.edu/time/>

Table 1. All available mid-eclipse times for the eclipsing binary Z Dra.

HJD(UTC) (days)	BJD(TDB) (days)	Error ^a (days)	Cycle	$O - C$ (days)	Method ^b	Type ^c	Author/Observer	Source
2411487.4696	2411487.46998	0.005*	-23583.0	0.05598	P	pri	Dugan R.S.	1915MNRAS...75...702
2412859.8414	2412859.84178	0.005*	-22572.0	0.06413	P	pri	Dugan R.S.	1915MNRAS...75...702
2414392.3702	2414392.37058	0.005*	-21443.0	0.05231	P	pri	Dugan R.S.	1915MNRAS...75...702
...
2456601.0307	2456601.03147	0.003*	9651.5	0.04699	CC	sec	Nelson R.H.	2014IBVS...6092
2456632.9278	2456632.92857	0.0003	9675.0	0.04444	CC	pri	Nelson R.H.	2014IBVS...6092
2456775.4604	2456775.46117	0.0003	9780.0	0.04679	CC	pri	Yuan et al.	the present paper

^a An assumed error is marked with an asterisk (*).

^b CC = CCD, E = Photoelectric, P = Photoplate, V = visual, PG = Photo Graphic, F = Series of exposures.

^c pri = primary mid-eclipse time, sec = secondary mid-eclipse time.

(This table is available in its entirety in machine-readable and Virtual Observatory (VO) forms in the online journal. A portion is shown here for guidance regarding its form and content.)

In equation (4), σ_i is the uncertainties of the $O - C$ data y_i .

Stepping through e_3 and T_3 , and finally P_3 , we obtain χ^2 as a function of P_3 , i.e., $\chi^2(P_3)$. Normalised by the best $\chi^2(P_3)$ (i.e., $\chi_{best}^2 \equiv \chi^2(P_{3,best}) = 5429.4$), we obtain a power spectrum (Zechmeister & Kürster 2009; Cumming et al. 1999; Cumming 2004),

$$p(P_3) \equiv \frac{\chi_0^2 - \chi^2(P_3)}{\chi_{best}^2}, \quad (7)$$

where the constant $\chi_0^2 (= 58422.1)$ is the best-fit statistic of a fit of a parabola to the data. The one-dimensional periodogram is shown in Fig. 2(a), and peaks at $P \approx 20$, ~ 30 and ~ 60 yr, suggesting three companions with periods of ~ 60 , ~ 30 and ~ 20 yr (hereafter, referred to as Z Dra (AB)C, D and E, respectively). In addition, three smaller peaks near 14.1, 12.1 and 9.5 yr are also seen. The best fit corresponding to the most significant peak is plotted in Fig. 2(b), and listed in the second column (Solution 1) of Table 2.

We also use a quadratic plus two-LTT ephemeris to fit the $O - C$ data. We search for the best period in 40-90 yr with one LTT term, and the other LTT term in 5-35 yr. The linearized Keplerian fitting method (Yuan & Şenavcı 2014; Beuermann et al. 2012), which is very similar to the one-dimensional periodogram analysis above, is used to calculate a two-dimensional periodogram. The constraints on the two orbital periods are shown in Fig. 3(a). The χ^2 contour levels of 1.01, 1.1, 1.3, 1.7, 2.2, 2.5, 3.0, 4.0 and 5.0 have been normalized by division of the globally minimum $\chi_{global}^2 = 1632.5$. The best fit corresponding to χ_{global}^2 is plotted in Fig. 3(b), and listed in the third column (Solution 2) of Table 2.

Although the residuals of Solution 2 decrease from $\sim \pm 0.002$ d in Fig. 2(b) to $\sim \pm 0.001$ d in Fig. 3(b), cyclic variations are still visible. The semi-amplitude of 0.01 d is two times the mean uncertainty, suggesting other companion(s). The least-squares fit to the 802 mid-eclipsing times involves thirteen free parameters, three for the second-order polynomial in the ephemeris, and five orbital elements (P_k , e_k , ω_k , T_k , and $a_k \sin i_k / c$) for each companion. If all parameters are free, the number of degrees of freedom (DOF) is therefore 789. For the grid search in the (P_3, P_4) plane, the DOF is 2. In Fig. 3(a), the contour levels of 1.01 and 1.1 have increments $\Delta\chi^2$ of $0.01\chi_{global}^2 = 16.3$ and $0.1\chi_{global}^2 = 163$,

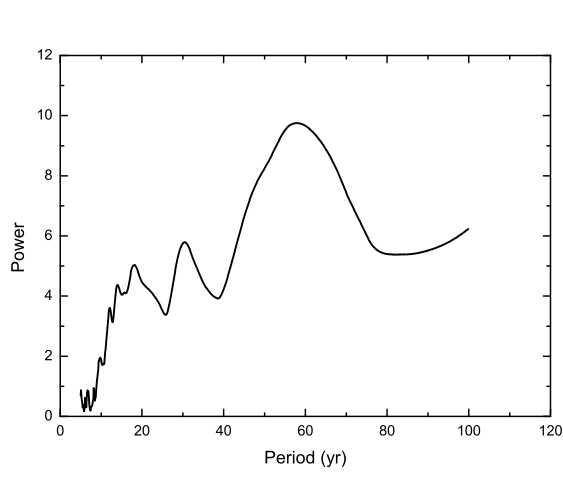
corresponding to confidence levels of 99.97% and 100% based on the probability distribution as a function of $\Delta\chi^2$ and 2 DOF (Beuermann, Dreizler & Hessman 2013). But We would like to remind the reader that the Solution 2 is unacceptable with $\chi_{global}^2 = 1632.5$ for 789 DOF (Bradt 2004). It is highly unlikely that the uncertainties of 802 data are generally underestimated since we have used slightly larger uncertainties for most data. We therefore conclude that the two-companion model is inadequate to describe the data. We should adopt a three-companion model or a four-companion model. In fact, the global χ^2 minimum in Fig. 3(a) suggests two companions with periods of ~ 60 and ~ 30 yr, while the local χ^2 minimum below reveals two companions with periods of ~ 60 and ~ 20 yr. Both minima reveal the companion with period of ~ 60 yr. In total, the two remarkable minima in the two-dimensional periodogram show three companions, i.e., Z Dra (AB)C, D and E. Furthermore, the two-dimensional periodogram also suggests other three possible companions with periods of ~ 15 , ~ 12 and ~ 9.5 yr.

In order to derive the orbital parameters of N_c companions, an ephemeris including a quadratic and N_c LTT terms is used to fit the $O - C$ values:

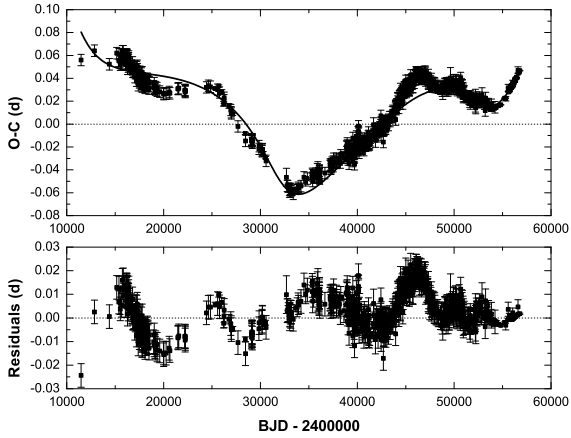
$$O - C = C_0 + C_1 \times t + C_2 \times t^2 + \sum_{k=3}^{N_c+2} \frac{a_k \sin i_k}{c} \cdot \left[\frac{1 - e_k^2}{1 + e_k \cos \nu_k} \sin(\nu_k + \omega_k) + e_k \sin \omega_k \right], \quad (8)$$

First, we use three LTT terms (i.e., $k = 3, 4, 5$) in equation (8), corresponding to three companions with periods near 60, 30 and 20 yr, respectively. We adopt an implementation of the nonlinear least-squares Levenberg-Marquardt fitting algorithm (Markwardt 2009). The best fit and corresponding χ^2 are listed in the fourth column (Solution 3) of Table 2, and plotted in Fig. 4. The solution yields the orbital periods of 59.48, 29.76 and 20.08 yr for the three outer companions, suggesting a near 6:3:2 mean-motion resonances (MMRs).

As shown in the bottom panel of Fig. 4, the residuals of Solution (3) seem to show cyclic variations. But the signal disappears after BJD 2452000. This may be due to the large weights and the short time coverage of the photoelectric and CCD points. Instead of fitting the residuals, an inner companion with a short orbital period of $P_6 < 16$ yr (hereafter, Z Dra (AB)F) as well as the three outer ones



(a)

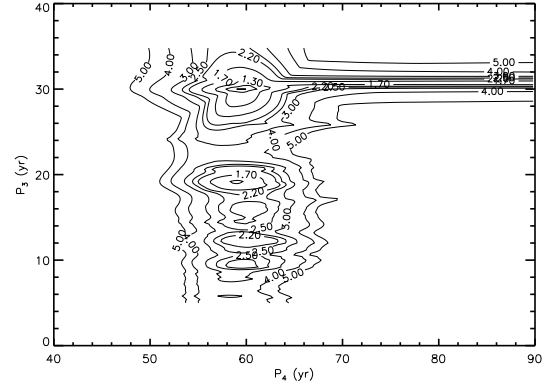


(b)

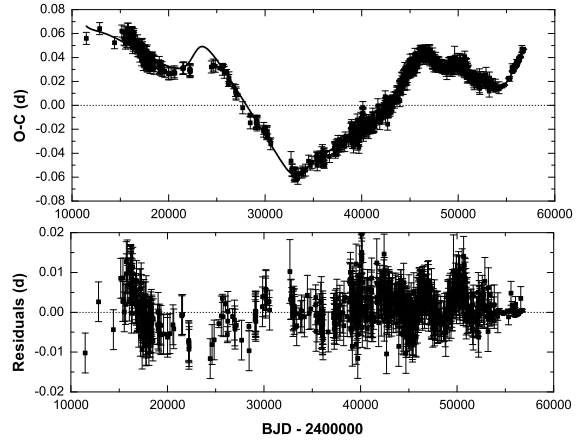
Figure 2. The one-companion fit to the eclipse-timing variations of Z Dra. (a) The normalized power spectrum of Z Dra. (b) The best fit for the globally maximum power (i.e., the globally minimum χ^2) in the top panel.

(i.e., Z Dra (AB)C, D and E) is used to fit the original $O - C$ data simultaneously. The best fit is plotted in Fig. 5, and listed in the fifth column (Solutions 4) of Table 2. The orbital period of Z Dra (AB)F is 9.18 yr, which places the inner companion close to 6:3:2:1 MMRs with the three outer companions. The reduced $\chi^2_\nu = 1.38$ ($\chi^2 = 1073.2$ for 779 DOF) improves greatly, but is still high. In addition, the Levenberg-Marquardt fits also converge toward Solutions 5 and 6, which give two local χ^2 minima. We note, however, that the orbital parameters of the three outer companions in Solutions (4-6) differ from each other.

Finally, we try to fit the $O - C$ data with six LTT terms simultaneously, but the fit can not converge. This is consistent with our predictions: in Solutions (4-6), $a_6 \sin i_6 = 0.32 - 0.74$ au (i.e., $\sim 0.002 - 0.004$ light day) can induce LTT signals of only 0.002-0.004 d, which are at the noise level of



(a)



(b)

Figure 3. The two-companion fit to the eclipse-timing variations of Z Dra. (a) Two-dimensional periodogram of Z Dra. The χ^2 contours of 1.01, 1.1, 1.3, 1.7, 2.2, 2.5, 3.0, 4.0 and 5.0 have been normalized by division of the globally minimum $\chi^2 = 1632.5$. (b) the best fit for the globally minimum χ^2 in the top panel.

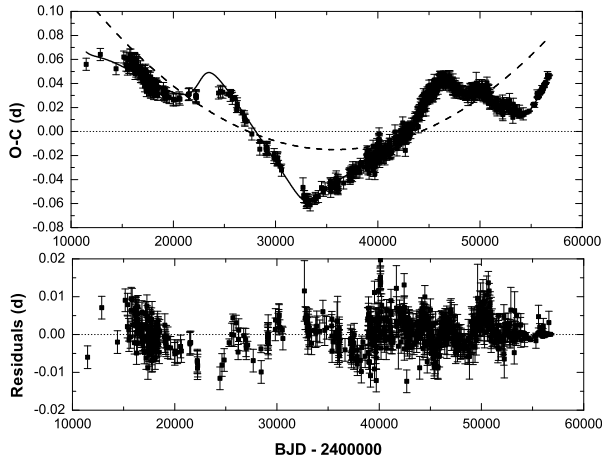
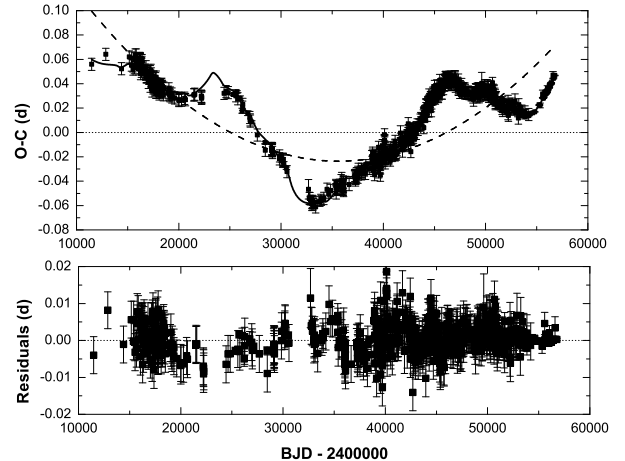
the $O - C$ data. Alternatively, we have not chosen proper starting values for all 33 model parameters. It is difficult to find 33 appropriate parameters as the initial input for the Levenberg-Marquardt technique.

3 DYNAMICAL STUDY

Our LTT fits provide all orbital parameters of the companions except for the inclinations i_k ($k = 3, 4, \dots$). Based on an assumed inclination of one companion, its mass (m_k) can be derived (see Yuan & Şenavcı 2014 for details). For example, if the orbital inclinations of all companions are 90.0° , they would have minimum masses (see Table 2). In general, the most outer companion Z Dra (AB)C has the minimum mass of $0.7 - 0.9 M_\odot$, whereas other companions are M dwarfs with masses of $0.1 - 0.3 M_\odot$. Furthermore, the orbitally angular configuration of one external companion relative to the most inner one is determined by both i_k and θ_k (the

Table 2. The best-fitting parameters for the LTT orbits of Z Dra.

parameter	Solution 1	Solution 2	Solution 3	Solution 4	Solution 5	Solution 6
C_0 (d)	0.2685 ± 0.0013	0.2572 ± 0.0015	0.2415 ± 0.0018	0.2448 ± 0.0016	0.2429 ± 0.0011	0.2391 ± 0.0021
C_1 ($\times 10^{-3}$ d yr $^{-1}$)	-6.096 ± 0.025	-5.559 ± 0.030	-5.560 ± 0.032	-5.507 ± 0.031	-5.465 ± 0.024	-5.4626 ± 0.028
C_2 ($\times 10^{-5}$ d yr $^{-2}$)	3.097 ± 0.011	2.838 ± 0.014	2.850 ± 0.015	2.825 ± 0.014	2.804 ± 0.012	2.792 ± 0.019
P_6 (yr)				9.18 ± 0.03	12.63 ± 0.05	15.41 ± 0.07
T_6 (BJD)				2400781 ± 169	2403528 ± 222	2402741 ± 245
e_6				0.639 ± 0.087	0.696 ± 0.134	0.434 ± 0.058
$a_6 \sin i_6$ (au)				0.36 ± 0.04	0.34 ± 0.04	0.71 ± 0.09
ω_6 (deg)				208.4 ± 8.1	184.6 ± 9.8	311.1 ± 11.7
m_6 (M_\odot , $i_6 = 90^\circ$)				0.13 ± 0.01	0.10 ± 0.01	0.19 ± 0.03
P_5 (yr)			20.14 ± 0.08	20.04 ± 0.05	20.16 ± 0.06	20.42 ± 0.10
T_5 (BJD)			2401029 ± 204	2401308 ± 137	2400974 ± 165	2400162 ± 266
e_5			0.935 ± 0.083	0.723 ± 0.021	0.755 ± 0.024	0.789 ± 0.039
$a_5 \sin i_5$ (au)			0.85 ± 0.09	1.42 ± 0.07	1.32 ± 0.09	1.08 ± 0.07
ω_5 (deg)			35.5 ± 5.8	66.4 ± 8.2	48.9 ± 6.3	11.0 ± 5.3
m_5 (M_\odot , $i_5 = 90^\circ$)			0.19 ± 0.02	0.33 ± 0.02	0.30 ± 0.02	0.24 ± 0.02
P_4 (yr)		29.80 ± 0.08	30.02 ± 0.09	29.12 ± 0.14	29.70 ± 0.17	29.82 ± 0.12
T_4 (BJD)		2400412 ± 173	2410423 ± 272	2404604 ± 170	2402940 ± 256	2403324 ± 189
e_4		0.440 ± 0.014	0.293 ± 0.041	0.789 ± 0.082	0.596 ± 0.062	0.572 ± 0.056
$a_4 \sin i_4$ (au)		2.10 ± 0.03	1.96 ± 0.13	1.50 ± 0.10	1.23 ± 0.08	1.95 ± 0.12
ω_4 (deg)		283.3 ± 4.9	343.8 ± 6.7	152.7 ± 3.8	108.7 ± 13.7	119.4 ± 7.2
m_4 (M_\odot , $i_4 = 90^\circ$)		0.38 ± 0.01	0.35 ± 0.03	0.27 ± 0.02	0.21 ± 0.02	0.35 ± 0.03
P_3 (yr)	57.90 ± 0.09	59.49 ± 0.13	59.37 ± 0.10	59.64 ± 0.11	59.84 ± 0.13	59.86 ± 0.14
T_3 (BJD)	2410922 ± 98	2401330 ± 112	2411313 ± 146	2408646 ± 81	2408678 ± 101	2410433 ± 139
e_3	0.390 ± 0.004	0.623 ± 0.018	0.510 ± 0.024	0.610 ± 0.012	0.570 ± 0.016	0.580 ± 0.020
$a_3 \sin i_3$ (au)	5.57 ± 0.08	6.10 ± 0.07	5.88 ± 0.14	6.90 ± 0.06	6.64 ± 0.09	6.38 ± 0.08
ω_3 (deg)	223.4 ± 1.3	76.3 ± 3.9	242.1 ± 3.5	200.0 ± 0.9	201.7 ± 1.3	228.9 ± 2.1
m_3 (M_\odot , $i_3 = 90^\circ$)	0.70 ± 0.01	0.77 ± 0.01	0.74 ± 0.01	0.90 ± 0.01	0.85 ± 0.01	0.81 ± 0.01
χ^2	5429.4	1632.5	1266.2	1073.2	1164.3	1168.2


Figure 4. $O - C$ diagram of Z Dra. The overplotted solid line denotes the best fit (Solution 3) with an ephemeris including three LTT terms and a quadratic trend, and the dashed line represents the quadratic part in the ephemeris. The residuals of the best fit are displayed in the lower panel.

Figure 5. The same as in Fig. 4. but for Solution (4).

angle between their ascending nodes in the sky plane, see Fig. 6). Therefore, the configuration of an eclipsing binary with n LTT companions is determined by $2n - 1$ angular

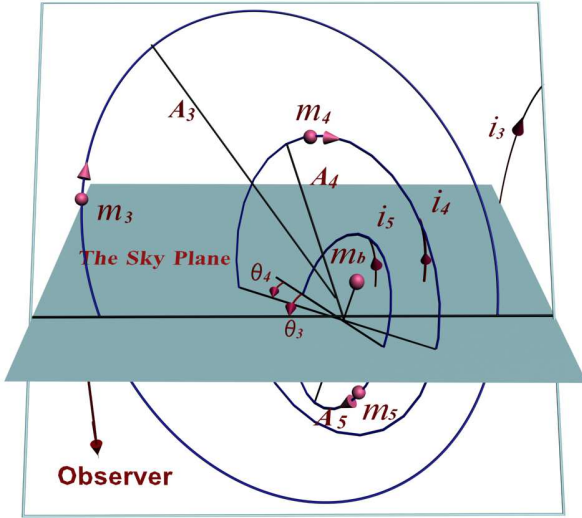


Figure 6. Schematic positions of the eclipsing binary (m_b) and its three companions ($m_{3,4,5}$) with respect to the tangent plane of the sky. $i_{3,4,5}$ denote the orbital inclinations of $m_{3,4,5}$, respectively. $A_{3,4,5}$ refer to orbital semi-major axes in Jacobian coordinates. For instance, A_3 is orbital semi-major axis of m_3 around the total barycenter of all internal bodies (i.e., $m_{4,5,b}$). (A color version of this figure is available in the online journal.)

parameters. For simplicity, the central eclipsing binary was treated as a single object (m_b) with a mass equal to the sum of the masses of both components. In the case of Z Dra, $m_b = 1.90M_\odot$ (Terrell 2006).

In order to check the stability of the system, the variable-step Runge-Kutta-Nystrom algorithm (Dormand, El-Mikkawy & Prince 1987) implemented in the orbit integration code LTTBODIES (Yuan & Şenavcı 2014) is used in our dynamic simulations. First, only the three outer companions as well as the eclipsing pair are considered. We adopt a grid resolution of 2° to search the angular space of five dimensions. The results show that no orbital configurations can survive for 200 yr. Then, the possible inner companion (with the period of 9.18 yr) is included in these simulations. In order to reduce the computational cost of the simulations, a lower grid resolution of 5° is used in the seven-dimensional angular space. However, the system is yet unstable in a series of orbital configurations. Just as mentioned above, there may be more than one short-period ($P_6 < 16$ yr) companions. However, the more companions we consider, the more intensive the computation is. Such numerical simulations are beyond current computational capabilities.

4 DISCUSSIONS AND CONCLUSIONS

A detailed $O - C$ analysis of Z Dra is performed using all available mid-eclipse times covering 124 yr, together with a new mid-eclipse time obtained in this paper. The $O - C$ diagram shows complex behavior, providing invaluable information about the multiple-companion system. The quadratic trend represents a continuous observed period increase with a rate of $dP/dt = 2.1 \times 10^{-7} \text{ d yr}^{-1}$, which is a typical value

for many contact binary stars (see e.g., Qian 2001, 2003, 2008). A possible physical mechanism that can explain the period increase is mass transfer from the secondary component to the primary one.

We have searched the $O - C$ data for periodicities between 5 and 100 yr, and three or four periods are found to have simple ratios. Even if we do not discard 14 mid-eclipse times, the result of the 6:3:2:1 MMRs is not affected. The quasi-sinusoidal variations can also be attributed to the magnetic activity cycles (Applegate 1992; Yuan & Qian 2007). In the case of Z Dra, no strong magnetic activity, however, is reported in the literature (e.g., Eker et al. 2008). This indicates three or four companions in the resonant configuration rather than magnetic activity cycles. Actually, many stable N -body systems are in resonant configurations.

Since $\sum_{i=1}^{802} w_i = 1$, $\sqrt{\chi^2/W}$ can be regarded as the root-mean-square (rms) scatter around the best fit (Marsh et al. 2014). In Solutions (2-6), $\sqrt{\chi^2/W} = 0.0012 - 0.0015$ d. On the other hand, the semi-amplitude of the LTT signals of component k is given by $(a_k \sin i_k)/c$, where c is the speed of light. In the cases of Solutions (2-6), the semi-amplitudes of the LTT signal of Z Dra (AB)C, D, and E are 0.035 – 0.039, 0.007 – 0.012, and 0.006 – 0.008 d, respectively, which are 2-13 times the rms scatter. But for Z Dra (AB) F, the LTT signal with the semi-amplitude of 0.002 – 0.004 d is about equal to the rms scatter. Therefore, we are confident of Z Dra (AB)C, D, and E orbiting around Z Dra AB, and predict other possible companion(s) with (a) period(s) shorter than 16 yr.

In all solutions, Z Dra (AB)E has an eccentricity of $e_5 > 0.7$. Such high eccentricities are seen for some companions around other eclipsing binaries, such as SZ Her (Hinse et al. 2012), QS Vir (Horner et al. 2013) and RZ Dra (Hinse et al. 2014). We also note $a_5 \sin i_5 > a_4 \sin i_4$ in Solution (5). This does not necessarily imply a cross-orbit architecture since the Jacobian semi-axis of $A_k = a_k \cdot (\sum_{i=k, \dots, 6, b} m_i)/m_k$ ($k = 4, 5$). Nevertheless, we should keep in mind that these abnormal characteristics of Z Dra (AB)E as well as the appearance of Z Dra (AB)F may be resulted from the low-precision data, which can not provide tight constraints on the properties of the internal companion(s).

We have attempted to find stable angular configurations of the companions, but neither the number of the companions nor their orbital parameters are determined accurately. Ultimately, we fail to find any stable angular configurations. We therefore encourage follow-up observations of this system to obtain high-precision mid-eclipse times covering as long baseline as possible, which will help to guide searches for stable angular configurations. In spite of the failure, all solutions in this paper reveal three or four companions orbiting around Z Dra AB in a near mean-motion resonances.

ACKNOWLEDGEMENTS

We would like to thank Kreiner J. M. for his data and the anonymous referee for some constructive suggestions. This research has also made use of the Lichtenknecker-Database of the BAV, operated by the Bundesdeutsche Arbeitsgemeinschaft für Veränderliche Sterne e.V. (BAV). The computations were carried out at National Supercomputer

Center in Tianjin, and the calculations were performed on TianHe-1(A). This work is supported by the National Natural Science Foundation of China (NSFC) (No. U1231121) and the research fund of Ankara University (BAP) through the project 13B4240006.

REFERENCES

- Applegate J. H., 1992, *ApJ*, 385, 621
Beuermann K., Dreizler S., Hessman F. V., Deller J., 2012, *A&A*, 543, 138
Beuermann K., Dreizler S., Hessman F. V., 2013, *A&A*, 555, 133
Bradt H. 2004, *Astronomy Methods*, Cambridge Univ. Press, Cambridge, p.170
Ceraski A. V., 1903, *Astron. Nach.*, 161, 159
Cumming A., 2004, *MNRAS*, 354, 1165
Cumming A., Marcy G. W., Butler R. P., 1999, *ApJ*, 526, 890
Dormand J. R., El-Mikkawy M. E. A., Prince P. J., 1987, *IMA J. Numer. Anal.*, 7, 423
Duffett-Smith P., Zwart J., 2011, *Practical Astronomy with your Calculator or Spreadsheet*, Cambridge Univ. Press, Cambridge, p.31
Dugan R. S., 1915, *MNRAS*, 75, 702
Eastman J., Siverd R., Gaudi B. S., 2010, *PASP*, 122, 935
Eker Z. et al., 2008, *MNRAS*, 389, 1722
Giuricin G., Madirossian F., Mezzetti M., 1983, *ApJS*, 52, 35
Hinse T. C., Goździewski K., Lee J. W., Haghighipour N., Lee C.-U., 2012, *AJ*, 144, 34
Hinse T. C., Horner J., Lee J. W., Wittenmyer R. A., Lee C.-U., Park J.-H., Marshall J. P., 2014, *A&A*, 565, 104
Horner J., Wittenmyer R. A., Hinse T. C., Marshall J. P., Mustill A. J., Tinney C. G., 2013, *MNRAS*, 435, 2033
Irwin J. B., 1952, *ApJ*, 116, 211
Kreiner J. M., Kim C.-H., Nha, I.-S., 2001, *An Atlas of O C C Diagrams of Eclipsing Binaries* (Krakow: Wydawnictwo Naukowe Akademii Pedagogicznej)
Kwee K. K., van Woerden H., 1956, *Bull. Astron. Inst. Netherlands*, 464, 327
Markwardt C. B., 2009, in Bohlender D. A., Durand D., Dowler P., eds, *ASP Conf. Ser.*, Vol. 411, *Astronomical Data Analysis Software and Systems XVIII*. Astron. Soc. Pac., San Francisco, p. 251
Marsh T. R., Parsons S. G., Bours M. C. P., Littlefair S. P., Copperwheat C. M., Dhillon V. S., Breedt E., Cáceres C., Schreiber M. R., 2014, *MNRAS*, 437, 475
Nelson R. H., 2014, *Inf. Bull. Var. Stars*, 6092
Qian S.-B., 2001, *MNRAS*, 328, 914
Qian S.-B., 2003, *MNRAS*, 342, 1260
Qian S.-B., 2008, *AJ*, 136, 2493
Struve O., 1947, *ApJ*, 106, 92
Terrell D., 2006, *Inf. Bull. Var. Stars*, 5742
Yuan J. Z., Qian S. B., 2007, *ApJ*, 669, L93
Yuan J. Z., Şenavcı H. V., 2014, 439, 878
Zechmeister M., Kürster M., 2009, *A&A*, 496, 577